Engineering Conferences International
ECI Digital Archives

The 14th International Conference on Fluidization
– From Fundamentals to Products

Refereed Proceedings

2013

Reactivating the CO2 Capture Capacity of Exhausted Ca-Based Sorbent Particles for Fluidized Bed Calcium Looping Application (Double Looping)

Antonio Coppola
University of Naples "Federico II", Italy

Fabio Montagnaro
University of Naples "Federico II", Italy

Piero Salatino
University of Naples "Federico II", Italy

Fabrizio Scala
Institute for Research on Combustion, National Research Council, Italy

Follow this and additional works at: http://dc.engconfintl.org/fluidization_xiv

Part of the Chemical Engineering Commons

REACTIVATING THE CO_2 CAPTURE CAPACITY OF EXHAUSTED Ca-BASED SORBENT PARTICLES FOR FLUIDIZED BED CALCIUM LOOPING APPLICATION (DOUBLE LOOPING)

Antonio Coppola[a], Fabio Montagnaro[b]*, Piero Salatino[a] and Fabrizio Scala[c]

[a]Department of Chemical Engineering, University of Naples "Federico II", Piazzale Vincenzo Tecchio 80, 80125 Napoli, Italy
[b]Department of Chemical Sciences, University of Naples "Federico II", Complesso Universitario di Monte Sant'Angelo, 80126 Napoli, Italy
[c]Institute for Research on Combustion, National Research Council, Piazzale Vincenzo Tecchio 80, 80125 Napoli, Italy

*T: 39-081-674029; F: 39-081-674090; E: fabio.montagnaro@unina.it

ABSTRACT
The aim of this work was to study the hydration-reactivation behaviour of spent sorbents from a calcium looping (CaL) process. The changes of the sorbent properties induced by hydration, the regeneration of the CO_2 capture capacity and the attrition tendency of the material once reused in the CaL cycle were investigated. Results suggested that the sorbent should be hydrated for times as short as possible compatible with complete chemical hydration. In fact, long hydration times bring about cramming (chemical sintering) phenomena, lower enhancement of the active porosity, increased attrition tendency and reduced reactivation.

INTRODUCTION
Global warming due to anthropogenic CO_2 emissions is stimulating the development of novel combustion and gasification technologies ready for carbon capture and sequestration (1,2). The calcium looping (CaL) cycle, illustrated in Fig. 1, is based on the alternated temperature-swing uptake (in a fluidized bed - FB- carbonator) and release (in a FB calciner) of carbon dioxide from a calcium-based sorbent (e.g., limestone). This technology has reached the maturity of the demonstration stage. Reviews on this topic can be found in (3,4). In the carbonator, CO_2 in the flue gas is captured by CaO at around 650–700°C following an exothermic reaction. Thus, the carbonator emits a CO_2-depleted flue gas and a spent sorbent stream (a $CaCO_3$/CaO mixture, since carbonation is far from being complete) that can be fed to the calciner for the endothermic regeneration at around 900–950°C. This step yields a CO_2-rich flue gas (ready for further processing and storage) and regenerates the CaO-based sorbent. The CO_2 capture capacity and rate of the sorbent are progressively decreased by deactivation phenomena occurring over iterated looping, mainly due to sintering (5). Another issue is the competition between CO_2 and SO_2 in the flue gas (6–8). It is well known that CaO-based sorbents quickly react with SO_2, most often according to a core-shell conversion pattern (9,10). Sulphation brings about a loss and deactivation of Ca otherwise available for CO_2 capture. Moreover, limestone-based sorbents undergo attrition/fragmentation phenomena during FB processing. These phenomena result in the change of the granulometric (and residence time) distribution of the sorbent in the reactor and in a net calcium loss

from the circulating loop as elutriable fines. Sorbent attrition, which has been thoroughly characterized with reference to FB desulphurization ([11]–[13]), is relevant also in the context of CaL ([8],[14]–[16]). Optimal management of the CaL cycle implies continuous make-up of fresh limestone, to compensate for deactivation and attrition, and purge of spent sorbent. Landfilling of spent limestone is problematic due to the CaO-rich composition of this residue ([17]–[19]). The potential of spent sorbent from CaL as source of raw material in the cement manufacture is under scrutiny. An attractive alternative (from both environmental and economic points of view) is the regeneration of the CO_2 uptake capacity by hydration-induced reactivation of spent sorbent ([20]–[23]). This process, extensively studied in the past with reference to spent sorbents derived from flue gas desulphurization ([24]–[27]), is based on the CaO conversion to $Ca(OH)_2$, that gives rise to an increase in the molar volume from 16.9 cm^3 mol^{-1} (CaO) to 33.7 cm^3 mol^{-1} ($Ca(OH)_2$) and to a density decrease from 3.32 g cm^{-3} (CaO) to 2.20 g cm^{-3} ($Ca(OH)_2$). Swelling of CaO due to hydration is followed by dehydration of $Ca(OH)_2$ as the reactivated material is re-injected into the FB reactor. The resulting material is essentially CaO characterized by large specific surface area and porosity, and hence is more reactive toward acid gases (CO_2/SO_2) than the parent spent material. This *double looping* process is outlined in Fig. 2. Typically, spent sorbent retrieved from the calciner, hence CaO-rich, is hydrated (without the limiting effect related to the significant presence of a hard $CaCO_3$ shell). Eventually the reactivated sorbent is re-injected in the carbonator, with a twofold benefit: *i)* the $Ca(OH)_2$ endothermic dehydration reaction occurs in parallel with the exothermic carbonation; *ii)* feeding to the carbonator prevents excessive attrition related to fast dehydration and early sintering promoted by the high temperature in the calciner. Furthermore, the steam released during dehydration could have positive effects on the concurrent, if any, SO_2 capture from the flue gas in the carbonator. Hydration, however, might bring about enhanced attrition propensity of the reactivated material, even if only few results have been reported on this topic to date ([3],[28]). Hydration-induced reactivation of spent sorbents from CaL processes is a largely unexplored research topic that deserves investigation. Key issues are the changes in the sorbent physico-chemical properties induced by hydration, the regeneration of the CO_2 capture capacity, the influence of the sorbent regeneration on the attrition tendency of the material once reused in the looping cycle. These issues have been investigated in the present study with reference to an Italian limestone candidate for application in CaL.
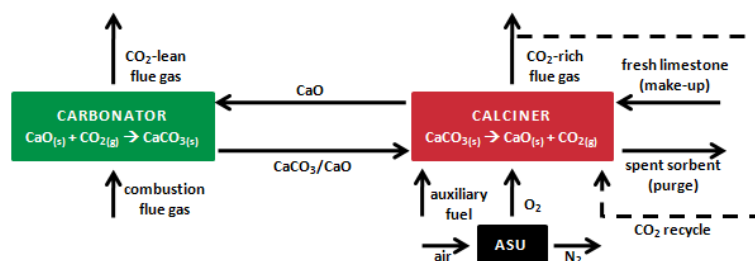

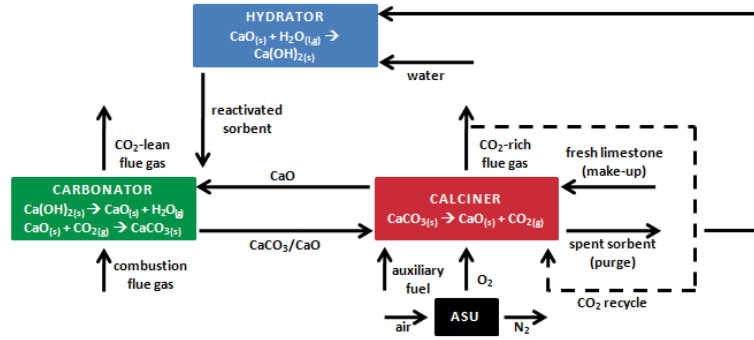**Figure 1:** The calcium looping process.

Figure 2: The *double looping* process for sorbent reactivation in CaL systems.

EXPERIMENTAL

The raw sorbent used in the tests was an Italian high-calcium limestone (Massicci). The test rig was a bubbling FB lab-scale reactor made of stainless steel, 40 mm ID. The reactor, operated at atmospheric pressure, was electrically heated and equipped with purposely designed filters that enabled time-resolved collection of elutriated fines at the exhaust. Details on the sorbent properties and the reactor are reported elsewhere ([8,16]). A cyclic sequence of five calcination/four carbonation stages was performed, starting with the raw sorbent (20 g sieved in the size range 0.4–0.6 mm). Each calcination step was carried out at 940°C for 20 min fluidizing the reactor at 0.7 m s^{-1} with a gas containing 70% CO_2 (balance air). Each carbonation step was carried out at 650°C for 15 min fluidizing the reactor at 0.6 m s^{-1} with a gas containing 15% CO_2 (balance air). Both calcination and carbonation stages lasted until completion. The CO_2 concentrations in the fluidizing gases were set at values corresponding to realistic operating conditions. The reactor, loaded with a bed of sand (150 g, 0.85–1 mm), was pre-heated to 940°C prior to feeding the batch of limestone. After calcination, the bed was rapidly discharged and the mixture sand/sorbent was separated by sieving. Then the reactor was cooled down to 650°C and loaded with sand. Once thermal equilibrium was approached, the sorbent was loaded. This procedure was repeated for each cycle. During the experiments, the rate of fines generation was measured (time-resolved data not reported for brevity), thus allowing to calculate the loss of elutriated material during each stage. The particle size distribution (PSD) of the sorbent was determined by sieving the bed material after each step. PSD analysis also allowed the determination of the mean Sauter diameter d_S of the distribution:

$$d_S = \frac{1}{\sum_i \frac{x_i}{d_i}} \tag{1}$$

where x_i is the mass fraction of particles having mean diameter d_i. The CO_2 capture capacity ξ after each carbonation stage was evaluated by working out the CO_2 concentration profiles at the exhaust (monitored by a continuous analyzer):

$$\xi = \frac{\int_0^t \left[W_{CO_2}^{in} - W_{CO_2}^{out}(t) \right] dt}{m_o} \tag{2}$$

where W is a mass flow rate and m_0 the initial mass of sorbent. Deactivated sorbent particles (spent sample S, retrieved after the 5th calcination) were reactivated by liquid-phase hydration in a thermostatic bath kept at 25°C. Batches of S (10 g) blended with a large excess of distilled water (water/solid weight ratio=25) were charged to sealed polyethylene bags and put in the thermostatic bath for curing times of 10, 30 and 60 min (samples water hydrated *WHY_10*, *WHY_30* and *WHY_60*, respectively). At the end of each hydration

experiment, samples were retrieved from the bags, vacuum filtered, left overnight at 110°C and then stored in a desiccator. Sorbent particles were characterized by means of the following experimental techniques: *i)* nonisothermal thermogravimetric (TG) analysis, from room temperature to 1000°C at a heating rate of 10°C min^{-1} under inert atmosphere (Ar) in a Netzsch STA409CD apparatus; *ii)* scanning electron microscopy (SEM) analysis, performed at magnifications up to 3000× in a FEI Inspect apparatus; *iii)* porosimetric analysis, carried out in a Micromeritics AutoPore IV apparatus for pore sizes ranging from 3 nm to 100 μm. In particular, TG analysis allowed calculating the hydration degree X_H:

$$X_H = \frac{n_{CaO}^{H}}{n_{CaO}^{S}}$$
(3)

where $n_{CaO}{}^{H}$ is the number of CaO moles reacted by hydration starting from the number of CaO moles present in *S* ($n_{CaO}{}^{S}$). Reactivated (*WHY*) material, sieved again in the particle size range 0.4–0.6 mm, was re-injected in the FB reactor for a new series of looping tests (now starting from the 5th carbonation step and ending to the 8th carbonation step), under the same operating conditions held before reactivation. Care was taken to make sure that the mass of CaO (not carbonated) available for the 5th carbonation, i.e. the first stage after reactivation, was the same as that remaining in the sample after the 5th calcination, i.e. the last stage before reactivation.

RESULTS AND DISCUSSION

Looping Cycles before Reactivation

The degree of CO_2 uptake after the 1st carbonation was ξ=0.05 g g^{-1}, and it decreased to ξ=0.03 g g^{-1} after the 4th carbonation due to sorbent deactivation. The poor values of ξ are related to the choice of a fairly high calcination temperature (940°C) coupled with the presence of a high CO_2 concentration (70%) during calcination, both factors promoting sorbent sintering, as it can be observed from the direct comparison with results obtained with the same sorbent under less severe operating conditions (16). A PSD having d_S=0.39 mm was observed after the 1st calcination, consistent with a limited shift toward smaller particle diameters with respect to the raw 0.4–0.6 mm sorbent. The amount of <0.1 mm in-bed sorbent fines was about 2% by mass. For the material retrieved after the 3rd carbonation, it was d_S=0.43 mm and the amount of in-bed sorbent fines was reduced (about 0.2% by mass). The sorbent attrition behaviour under looping conditions was evaluated by analyzing the elutriation data (Table 1). The loss of elutriated material during each calcination stage was 0.50±0.30% of the initial sorbent mass. Elutriation was more extensive during carbonation (1.00±0.37%). This interesting result highlights the major role of the particles' outer shell composition, with respect to that played by operating temperature. In fact, even if calcination is carried out at a higher temperature, at the beginning of this step sorbent particles are characterized by a hard $CaCO_3$-based shell, which would preserve particles from suffering extensive attrition. On the other hand, at the beginning of the "colder" carbonation stage sorbent particles are essentially made of CaO, softer and more prone to undergo attrition. No evident influence of the number of cycles on the elutriation tendency was observed (apart from the 1st cycle). After 4 complete calcination/carbonation cycles, the cumulative loss of elutriated fines was 5.36% of the inlet sorbent mass. When considering the elutriation values, one should take into account that, in this experimental

campaign: *i)* the sorbent was discharged from the bed after each stage, then cooled down and eventually re-injected into the hot bed for the following step; this procedure might have emphasized the thermal stresses suffered by the particles with respect to the case in which sorbent particles are continuously looped between the two reactors; *ii)* the duration of each stage was somewhat longer than those typical of large-scale looping applications ([29]). Both aspects could have affected the measured values of the elutriation rate as compared with those establishing under more realistic looping conditions.

Table 1: Loss of elutriated material (% of the initial sorbent mass) during each calcination and carbonation stage for raw and hydrated sorbent.

	calcination	carbonation
raw sorbent	1st: 0.20%	1st: 1.37%
	2nd: 0.79%	2nd: 0.72%
	3rd: 0.58%	3rd: 0.86%
	4th: 0.22%	4th: 0.62%
	5th: 0.30%	–
	range: 0.50±0.30%	range: 1.00±0.37%
	cumulative after 4 complete cycles: 5.36%	
WHY_10	–	5th: 0.27%
	6th: 0.74%	6th: 0.69%
	7th: 1.02%	7th: 1.14%
	8th: 0.75%	8th: 1.02%
	range: 0.88±0.14%	range: 0.70±0.43%
	cumulative after 3 complete cycles: 5.36%	
WHY_60	–	5th: 0.45%
	6th: 1.50%	6th: 1.14%
	7th: 0.52%	7th: 1.55%
	8th: 0.31%	8th: 1.15%
	range: 0.90±0.60%	range: 1.00±0.55%
	cumulative after 3 complete cycles: 6.17%	

Hydration-Induced Reactivation

TG analysis of the samples indicated that the *S* sorbent was mostly composed of CaO with some residual $CaCO_3$ (9.8%wt) that was left unconverted after the last (5th) calcination. The hydration degree of the water-reactivated samples increased from X_H=52.4% for *WHY_10* to X_H=55.2% for *WHY_60*, suggesting that chemical hydration is fairly fast and practically complete after the first 10 min. Further increase of X_H was likely hindered by the spent sorbent chemical (e.g., presence of residual $CaCO_3$) and physical (e.g., reduced porosity of the sintered *S* sample) properties. Fig. 3 reports selected SEM micrographs of the samples. Visual comparison of the morphology of *S* and *WHY* samples indicates that hydration brought about an increased degree of "softness" of the external surface of the samples. Quantitative considerations were obtained by analyzing porosimetric results, which were referred to the pore size range finer than 200 nm, since it has been reported in the literature ([30],[31]) that this is the range mostly affected by sintering/deactivation phenomena upon cycling. Therefore, in order for hydration to be effective, it must restore this "fine" porosity. The cumulative specific "fine" porosity was 65 mm^3 g^{-1} for *S*, and the hydration treatment was effective in increasing this porosity: 215 mm^3 g^{-1} (*WHY_10*), 198 mm^3 g^{-1} (*WHY_30*) and 181 mm^3 g^{-1} (*WHY_60*). The hydration treatment was

therefore able to induce an intraparticle pore regeneration process which underlies reactivation, due to the mechanisms discussed in the Introduction section. Moreover, the most pronounced increase in the <200 nm-porosity was observed just after 10 min-hydration, while longer hydration times resulted into a slight decrease in porosity with respect to that measured for *WHY_10*. This should be related to the competing effects of particle swelling (related to the chemical hydration process and, therefore, significant only during the initial hydration period) and low-temperature cramming/chemical sintering phenomena (relevant for longer hydration times and already observed in (24) when hydrating spent sorbents from flue gas FB desulphurization). Hydration results indicated that the most interesting reactivated sample is *WHY_10*, which was subjected to further CaL tests. To assess the effect of the hydration time, the performance of *WHY_10* was compared with that of the potentially less interesting *WHY_60* sample.
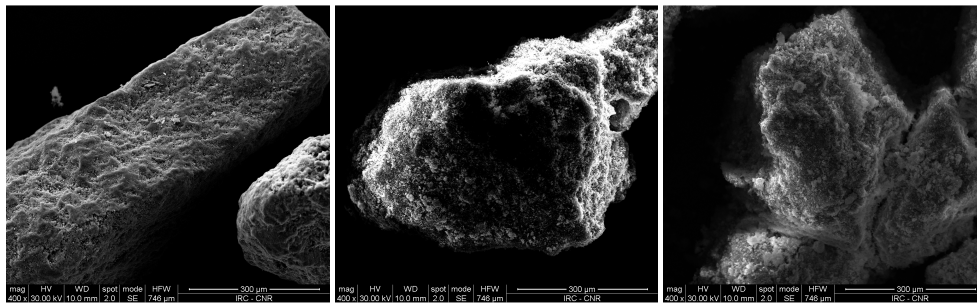

Figure 3: SEM micrographs for *S* (left), and *WHY* materials at two different times (middle, 10 min; right, 60 min).

Looping Cycles after Reactivation

Fig. 4 shows the ξ-values obtained for *WHY_10* and *WHY_60*, as a function of the number of carbonation stages and with reference to a ξ=0.03 g g^{-1} baseline, the value obtained after the 4th carbonation, i.e. the last carbonation before hydration. Results confirmed the effectiveness of the hydration treatment in regenerating the sorbent activity toward CO_2 capture. In particular, ξ decreased from 0.35 to 0.08 g g^{-1} (*WHY_10*) and from 0.19 to 0.03 g g^{-1} (*WHY_60*) along with the carbonation stages, highlighting that deactivation phenomena occurred also for the reactivated materials. *WHY_10* sample resulted more effective in CO_2 capture than *WHY_60*, and this should be mostly ascribed to the larger porosity achieved when hydrating for short hydration times, so to exploit the "chemical" hydration effect without suffering the long-term "physical" cramming effect. For *WHY_10*, PSD results showed that particle fragmentation was limited during the 5th carbonation (d_S=0.44 mm; cumulative mass of in-bed sorbent finer than 0.1 mm accounting for about 0.6% by mass). Fragmentation phenomena could be somewhat appreciated during the 6th calcination (i.e., the first calcination after reactivation), with d_S=0.38 mm and a fractional mass of fines of about 1.3%. This was ascribed to the more severe conditions to which the reactivated sorbent underwent upon its first calcination, in terms of thermo-mechanical shocks. For all the other cycles, the PSD did not show significant changes, even if a somewhat larger fragmentation tendency was observed along the cycles: altogether, d_S in the range 0.34–0.44 mm and an amount of fines in the range 0.6–1.5% were recorded. Similar considerations hold for *WHY_60*: d_S=0.44 mm and 0.6% fines after the 5th carbonation, d_S=0.40 mm and 1.0% fines after the 6th calcination and,

in general, d_S in the range 0.36–0.44 mm and an amount of in-bed fines in the range 0.3–1.3%. Table 1 reports elutriation data for the reactivated materials. The loss of elutriated material during each calcination and carbonation stage was 0.88±0.14% and 0.70±0.43%, respectively, for *WHY_10*, and 0.90±0.60% and 1.00±0.55%, respectively, for *WHY_60*. The cumulative loss of elutriated fines after 3 complete calcination/carbonation stages (therefore, discarding the datum relative to the 5th calcination) was 5.36% and 6.17% for *WHY_10* and *WHY_60*, respectively. These data: *i)* confirm the general trend concerning greater losses of elutriated material during carbonation, as already discussed; *ii)* highlight that soaking can induce a greater attrition tendency for *WHY_60* material; *iii)* reveal that hydration can moderately emphasize the sorbent attrition tendency when compared with the raw material. It can also be noted that the lower CO_2 capture capacities shown by *WHY_60* can determine a less-marked formation of a hard $CaCO_3$-based shell upon carbonation, and this effect partly adds on soaking in making *WHY_60* more attritable than *WHY_10*. These results highlight the relationships between CO_2 capture capacity, surface properties and attrition tendency. Altogether, results suggest that the sorbent should be hydrated for times long enough to get a substantially complete chemical hydration, but short enough to avoid soaking and cramming phenomena, lower enhancement in the active porosity, increased attrition tendency and reduced reactivation.
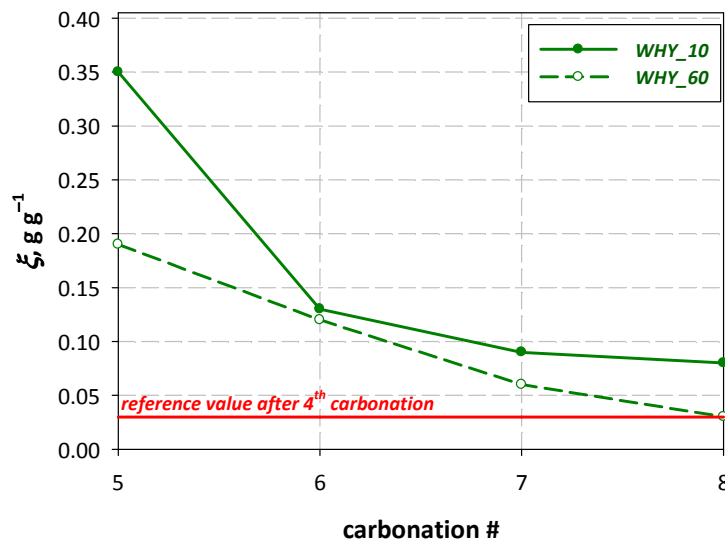

Figure 4: CO_2 capture capacity for the reactivated *WHY_10* and *WHY_60* samples as a function of the number of carbonation stages (the 5th carbonation is the first carbonation step after hydration).

NOTATION

d	particle diameter	[m]	t	time	[s]
d_S	mean Sauter diameter	[m]	W	CO_2 mass flow rate	[g s^{-1}]
m_0	initial mass of sorbent	[g]	x	mass fraction of particles	[g g^{-1}]
n_{CaO}^H	number of CaO moles reacted by hydration	[mol]	X_H	hydration degree	[mol mol^{-1}]
n_{CaO}^S	number of CaO moles present in the spent sample	[mol]	ξ	CO_2 capture capacity	[g g^{-1}]

REFERENCES

(1) F Li, LS Fan: *Energy Environ Sci* 1(2008)248–67.

(2) ES Rubin, H Mantripragada, A Marks, P Versteeg, J Kitchin: *Prog Energy Combust Sci* 38(2012)630–71.

(3) J Blamey, EJ Anthony, J Wang, PS Fennell: *Prog Energy Combust Sci* 36(2010)260–79.

(4) CC Dean, J Blamey, NH Florin, MJ Al-Jeboori, PS Fennell: *Chem Eng Res Des* 89(2011)836–55.

(5) M Alonso, N Rodríguez, B González, GS Grasa, R Murillo, JC Abanades: *Int J Greenh Gas Control* 4(2010)167–73.

(6) P Sun, JR Grace, CJ Lim, EJ Anthony: *Energy Fuels* 21(2007)163–70.

(7) GS Grasa, M Alonso, JC Abanades: *Ind Eng Chem Res* 47(2008)1630–5.

(8) A Coppola, F Montagnaro, P Salatino, F Scala: *Chem Eng J* 207–208(2012)445–9.

(9) EJ Anthony, DL Granatstein: *Prog Energy Combust Sci* 27(2001)215–36.

(10) F Montagnaro, P Salatino, F Scala: *Exp Therm Fluid Sci* 34(2010)352–8.

(11) F Scala, A Cammarota, R Chirone, P Salatino: *AIChE J* 43(1997)363–73.

(12) F Scala, F Montagnaro, P Salatino: *Energy Fuels* 21(2007)2566–72.

(13) F Montagnaro, P Salatino, F Scala, M Urciuolo: *Ind Eng Chem Res* 50(2011)9704–11.

(14) PS Fennell, R Pacciani, JS Dennis, JF Davidson, AN Hayhurst: *Energy Fuels* 21(2007)2072–81.

(15) A Charitos, C Hawthorne, AR Bidwe, S Sivalingam, A Schuster, H Spliethoff, G Scheffknecht: *Int J Greenh Gas Control* 4(2010)776–84.

(16) A Coppola, F Montagnaro, P Salatino, F Scala: *Combust Sci Technol* 184(2012)929–41.

(17) F Montagnaro, P Salatino, F Scala, G Bernardo, GL Valenti: *Fuel* 82(2003)2299–307.

(18) F Montagnaro, P Salatino, G Bernardo, A Telesca, GL Valenti: *Energy Fuels* 19(2005)1822–7.

(19) F Montagnaro, M Nobili, A Telesca, GL Valenti, EJ Anthony, P Salatino: *Fuel* 88(2009)1092–8.

(20) V Manovic, EJ Anthony: *Environ Sci Technol* 41(2007)1420–5.

(21) F Zeman: *Int J Greenh Gas Control* 2(2008)203–9.

(22) B Arias, GS Grasa, JC Abanades: *Chem Eng J* 163(2010)324–30.

(23) W Wang, S Ramkumar, S Li, D Wong, M Iyer, BB Sakadjian, RM Stanick, LS Fan: *Ind Eng Chem Res* 49(2010)5094–101.

(24) F Montagnaro, F Scala, P Salatino: *Ind Eng Chem Res* 43(2004)5692–701.

(25) F Montagnaro, F Pallonetto, P Salatino, F Scala: *AIChE J* 52(2006)4090–8.

(26) EJ Anthony, EM Bulewicz, L Jia: *Prog Energy Combust Sci* 33(2007)171–210.

(27) F Montagnaro, P Salatino, L Santoro, F Scala: *Chem Eng J* 162(2010)1067–74.

(28) V Materić, S Edwards, SI Smedley, R Holt: *Ind Eng Chem Res* 49(2010)12429–34.

(29) N Rodríguez, M Alonso, JC Abanades, A Charitos, C Hawthorne, G Scheffknecht, DY Lu, EJ Anthony: *Energy Procedia* 4(2011)393–401.

(30) PS Fennell, JF Davidson, JS Dennis, AN Hayhurst: *J Energy Inst* 80(2007)116–9.

(31) P Sun, JR Grace, CJ Lim, EJ Anthony: *Ind Eng Chem Res* 47(2008)2024–32.